

Thermodynamic properties of Zr_2Al under high pressure from first-principles calculations

X. L. Yuan^{a,b}, D. Q. Wei^{b,c,*}, Y. Cheng^{a,*}, Q. M. Zhang^c,
and Z. Z. Gong^d

^a College of Physical Science and Technology, Sichun University, Chengdu 610064, China

^b College of Life Science and and Biotechnology, Shanghai Jiaotong University, Shanghai 200240, China

^c State Key Laboratory of Explosion Science and Technology, Beijing Institute of Technology, Beijing 100081, China

^d Chinese Academy of Space Sciences, Beijing 100094, China

Received 10 July 2011; Accepted (in revised version) 5 August 2011

Published Online 8 November 2011

Abstract. The equations of state (EOS) and other thermodynamic properties of hcp structure Zr_2Al are studied using first-principles calculations based on the plane wave pseudopotential density functional theory method within the generalized gradient approximation (GGA) for exchange and correlation. It is demonstrated that the ratio c/a of about 1.208 is the most stable structure for the hcp Zr_2Al , which is consistent with the experimental data. Through the quasi-harmonic Debye model, in which the phononic effects are considered, the dependences of relative volume V/V_0 on pressure P , cell volume V on temperature T are successfully obtained. The variations of the Debye temperature Θ , the thermal expansion α , the Grüneisen parameter γ and the heat capacity C_v with pressure P and temperature T are investigated systematically in the ranges of 0–100 GPa and 0–1500 K.

PACS: 65.40.-b; 81.05.Bx

Key words: equations of state, thermodynamic properties, generalized gradient approximation, Zr_2Al

1 Introduction

The equation of state (EOS) and other thermodynamic properties for crystalline materials are fundamentally important in studying the high pressure physics of solids and applied sciences, which provide insight into the nature of solid state theories. Intermetallic compounds and ordered alloys recently attracted much attention as practical materials, zirconium-aluminum

*Corresponding author. *Email addresses:* dqwei@sjtu.edu.cn (D. Q. Wei); ycheng@scu.edu.cn (Y. Cheng)

alloys have potential application in aircraft turbine engines, medical, and the nuclear energy fields used as fuel-element-cladding materials due to their high strength, light weight, corrosion resistance and low neutron capture cross sections [1]. There are also numerous applications of zirconium-aluminum alloys as hydrogen getters in vacuum systems and microwave lasers. The zirconium-aluminum system is characterized by a number of intermetallic compounds which have been studied crystallographically by several investigators [2–10]. Especially, considerable work has been done to investigate the phase diagram and thermodynamic properties [11–16]. For example, Schneider *et al.* reported the free energies of formation of three compounds: $ZrAl_2$, Zr_2Al_3 , Zr_4Al_3 , measured by solution calorimetry at one temperature [17]; Kematick *et al.* studied the heats of formation of the zirconium-aluminum intermetallic compounds $ZrAl_3$, $ZrAl_2$, Zr_2Al_3 , $ZrAl$, Zr_5Al_4 , Zr_3Al_2 , Zr_5Al_3 [15]. However, to date few thermodynamic data have been reported for Zr_2Al system.

In this paper, the equations of state (EOS) and other thermodynamic properties of hcp structure Zr_2Al are investigated by applying the first-principles plane-wave method within the generalized gradient approximation correction (GGA) in the frame of density functional theory [18] based on the Cambridge Serial Total Energy Package (CASTEP) program [19,20] and the quasi-harmonic Debye model [22], which allows us to obtain all thermodynamics quantities from the calculated energy-volume points.

2 Method of calculation

2.1 Total energy electronic structure calculations

In the present electronic structure calculation, we apply the GGA for the exchange-correlation functional in the scheme of Perdew-Burke-Ernzerhof (PBE) [22] to describe the exchange and correlation potential. A plane-wave basis set with energy cut-off 360 eV is applied. Pseudo atomic calculations are performed for $Zr(4d^25s^2)$ and $Al(3s^23p^1)$. For the Brillouin-zone sampling, we use the $9 \times 9 \times 8$ Monkhorst-Pack mesh, where the self-consistent convergence of the total energy is at 1.0×10^{-6} eV/Atom. All the total energy electronic structure calculations are implemented through the CASTEP code [19,20].

2.2 Thermodynamic properties

To investigate the thermodynamic properties of the hcp structure Zr_2Al , the quasi-harmonic Debye model is adopted. Our calculations are implemented through the Gibbs code by Blanco *et al.* [21], which is used to obtain as much thermodynamic information as possible from a minimum set of (E, V) data. In the following, a brief description for this model is presented.

In the quasi-harmonic Debye model, the non-equilibrium Gibbs function $G^*(V; P, T)$ is written as following

$$G^*(V; P, T) = E(V) + PV + A_{vib}(V; T), \quad (1)$$

where $E(V)$ is the total energy per unit cell for Zr_2Al , PV corresponds to the constant hydrostatic pressure condition, A_{vib} is the vibrational Helmholtz. Considering the quasi-harmonic

approximation [23] and using the Debye model of phonon density of states, one can write A_{vib} as [24–26]

$$A_{vib}(\Theta; T) = nk_B T \left[\frac{9\Theta}{(8T)} + 3 \ln \left(1 - e^{-\frac{\Theta}{T}} - D\left(\frac{\Theta}{T}\right) \right) \right], \quad (2)$$

where $D(\Theta/T)$ represents the Debye integral, n is the number of atoms per formula unit. For an isotropic solid, Θ is in the form of

$$\Theta = \frac{\hbar}{K} \left[6n\pi^2 V^{\frac{1}{2}} \right]^{\frac{1}{3}} f(\sigma) \sqrt{\frac{B_s}{M}}, \quad (3)$$

where M is the molecular mass per unit cell, B_s is the adiabatic bulk modulus, approximated by the static compressibility [21]

$$B_s = \left(\frac{d^2 E(V)}{dV^2} \right). \quad (4)$$

And $f(\sigma)$ is given by Refs. [21, 25]. Consequently, the non-equilibrium Gibbs function $G^*(V; P, T)$ as a function of $(V; P, T)$ can be minimized with respect to volume V as

$$\left(\frac{\partial G^*(V; P; T)}{\partial V} \right)_{P, T} = 0. \quad (5)$$

By solving Eq. (5), one can get the thermal EOS of compound Zr_2Al . The isothermal bulk modulus B_T is expressed by [21]

$$B_T(P, T) = V \left(\frac{\partial^2 G^*(V; P, T)}{\partial V^2} \right)_{P, T}, \quad (6)$$

$$C_v = 3nk \left(4D(\Theta/T) - \frac{3\Theta/T}{e^{\Theta/T} - 1} \right), \quad (7)$$

$$\alpha = \frac{\gamma C_v}{B_T V}, \quad (8)$$

where γ is the Grüneisen parameter, which is defined as

$$\gamma = - \frac{d \ln \Theta(V)}{d \ln V}. \quad (9)$$

Applying the method, one has investigated the thermodynamic properties of a series of materials [27–30].

3 Results and discussion

In order to determine the equilibrium geometry of Zr_2Al , we do the following procedures. In the first step, we fix the ratio c/a , and take a series of different values of a and c to

calculate the total energies E . No constraints are imposed on the c/a ratio, that is, both lattice parameters a and c are optimized simultaneously. In the second step, this procedure is repeated over a wide range of the ratio c/a (i.e. 1.196, 1.200, 1.204, 1.208, 1.212, 1.216, 1.220, 1.224, 1.228). By these methods, we obtain the most stable structure of Zr_2Al at 0 K and 0 GPa corresponding to the axial ratio $c/a = 1.208$ and $a = 4.908 \text{ \AA}$, $c = 5.929 \text{ \AA}$ (see Fig. 1), and then fit the calculated $E-V$ data to the natural strain EOS [31], in which the pressure-volume relationship expanded as

$$P = 3B_0 \frac{V_0}{V} f_N \left[1 + \frac{3}{2}(B' - 2)f_N + \frac{3}{2} \left(1 + B_0 B'' + (B' - 2) + (B' - 2)^2 f_N^2 \right) \right], \quad (10)$$

where $f_N = \ln(V/V_0)$, which may be written as $f_N = 1/3 \ln(V/V_0)$ for hydrostatic compression. B and B_0 are hydrostatic bulk modulus and zero pressure bulk modulus, respectively. For truncation at third-order in the strain, the implied value of B'' is given by

$$B'' = \frac{-1}{B_0} [1 + (B' - 2) + (B' - 2)^2]. \quad (11)$$

The calculated zero pressure bulk modulus B_0 and the pressure derivation of bulk modulus B'_0 from the natural strain EOS are about 102.71 GPa and 3.700, respectively. Applying the quasi-harmonic Debye model to Zr_2Al , we have obtained $B_0 = 100.52$ GPa and $B'_0 = 3.736$ GPa, together with other experimental data [32] and theoretical results [33], all results are list Table 1. Applying the calculated elastic constants at zero pressure, i.e. $C_{11} = 178.3$ GPa, $C_{12} = 85.4$ GPa, $C_{13} = 51.2$ GPa, $C_{33} = 189.2$ GPa and $C_{44} = 57.7$ GPa [34], to the following formula of the zero-pressure bulk modulus B_0

$$B_0 = \frac{(C_{11} + C_{12})C_{33} - 2C_{13}^2}{C_{12} + C_{11} + 2C_{33} - 4C_{13}}. \quad (12)$$

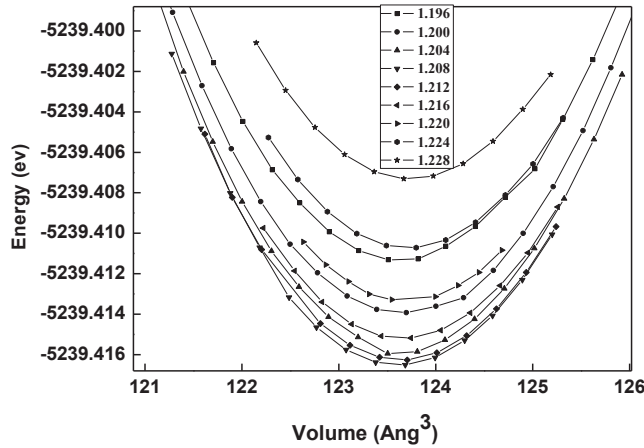


Figure 1: Total energy as function of primitive cell volumes corresponding to different c/a values.

We can obtain $B_0 = 102.10$ GPa. In the case, there is no constraint on the c/a dependence on lattice strain [35].

Table 1: The calculated structural parameters compared with experimental data and theoretical results.

	$a(\text{\AA})$	$c(\text{\AA})$	c/a	$V_0(\text{\AA}^3/\text{atom})$	$B_0(\text{GPa})$	B'_0	B''_0
Present work	4.908	5.929	1.208	20.61	102.71 ^a	3.00 ^a	-0.044 ^a
					100.52 ^b	3.736 ^b	-0.037 ^b
					102.10 ^c		
Exp. [32]	4.894	5.928	1.211	20.49			
Ref. [33]				20.38	98.10		

^a Obtained from the natural strain EOS [31].

^b Obtained from the Quasi-harmonic Debye model [21].

^c Obtained from the Eq. [12].

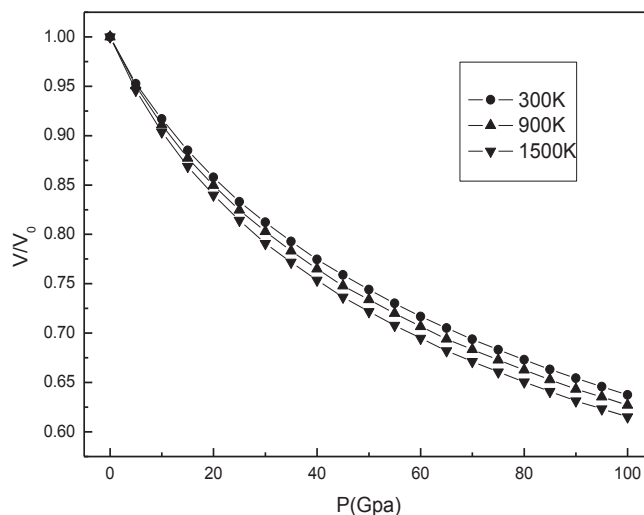


Figure 2: The pressure and temperature dependence of the relative volume V/V_0 of the Zr_2Al at the temperatures of 300 K, 900 K and 1500 K, respectively.

The pressure and temperature dependence of the relative volume V/V_0 of the Zr_2Al is shown in the Fig. 2. In order to further understand the physical change of Zr_2Al under pressure and temperature. It is seen that the relative volume V/V_0 decreases at the given temperature with the pressure increasing, and the higher temperature, the relative volume V/V_0 is the less at the same pressure. Therefore, this effect of decreasing temperature of the Zr_2Al is the same as the increasing pressure on Zr_2Al . The isobaric curves are presented in Fig. 3. It is seen that the volume varies rapidly as the temperature increase under lower pressure.

However, under higher pressure, it changes moderately and nearly linear. The compression behaviors of Zr_2Al correspond to the bonding situations in Zr_2Al . The atoms in the interlayers become closer when pressure increases, and the interactions between these atoms become stronger.

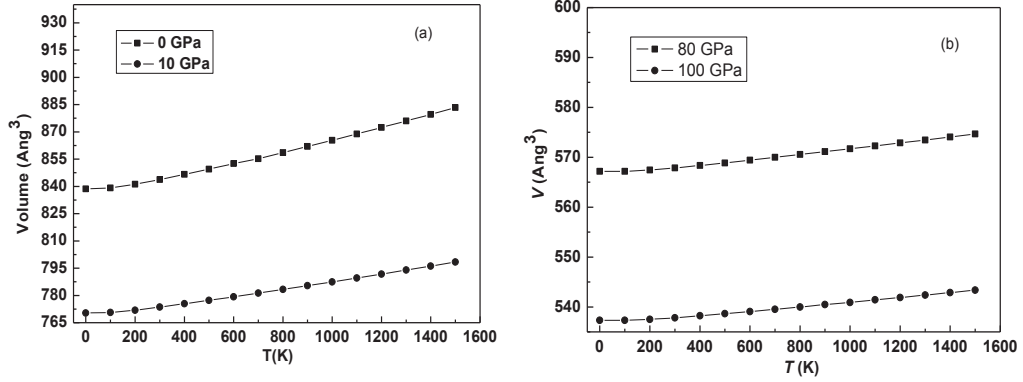


Figure 3: The volume-temperature relationship curves for Zr_2Al , and (a) under lower pressure, (b) under higher pressures.

As a fundamental parameter, the Debye temperature correlates with many physical properties of solids, such as specific heat, elastic constants, and melting temperature. At low temperatures the vibrational excitations arise solely from acoustic vibrations. Hence, at low temperatures the Debye temperature calculated from elastic constants is the same as that determined from specific heat measurements. From the elastic constants, one can obtain the elastic Debye temperature (Θ), expressed by following formulas [36]

$$\Theta = \frac{h}{k} \left(\frac{3nN_A\rho}{4\pi M} \right)^{\frac{1}{3}} v_m, \quad (13)$$

where h is Planck's constant, k is Boltzmann's constant, N_A is Avogadro's number, M is the molecule mass, ρ is the density, and the average sound velocity v_m is approximately presented by [37]

$$v_m = \left[\frac{1}{3} \left(\frac{2}{v_s^3} + \frac{1}{v_p^3} \right) \right]^{-\frac{1}{3}}, \quad (14)$$

where v_s and v_p are the transverse and longitudinal elastic wave velocities, respectively, which can be obtained from Navier's equation [36]

$$v_s = \sqrt{\frac{G}{\rho}}, \quad v_p = \sqrt{\frac{(B_s + \frac{4}{3}G)}{\rho}}, \quad (15)$$

where G is the shear modulus and B_s is the adiabatic bulk modulus.

By above-mentioned Eqs. (23)–(25), the Debye temperature calculated of Zr_2Al at 0 K temperature and 0 GPa is 396 K, closing to 388 K for Zr_3Al (L12) [33]. Unfortunately, no theoretical or experimental date is available for Zr_2Al .

The Debye temperature is also one key quantity in the quasiharmonic Debye model. In Fig. 4, we show the Debye temperature Θ as a function of temperatures at different pressures of $P = 0, 5, 10, 15$ and 20 GPa and pressure P at the temperatures of 300 K and 1200 K for Zr_2Al . For Fig. 4(a), it is shown that at low pressure, the Debye temperature Θ decreases significantly when the temperature changes from 0 to 1500 K. It can be noted that Θ decreases by 2.82%, 2.01%, 1.79% and 1.28% at the pressures of 0, 5, 10 and 15 GPa when the used temperature is from 0 to 600 K, respectively. And when the used pressure is from 0 to 15 GPa, Θ increases by 21.19%, 21.75% and 22.07% at the temperatures of 100, 300, and 400 K, respectively. As the pressure goes higher, the decreased magnitude of Θ becomes small. When the pressure approaches to 20 GPa, the variation of Θ is very small in the whole changed temperature range from 0 to 1500 K. Therefore, it can be concluded that the effect of the temperature on the Debye temperature Θ is not as important as that of the pressure on Θ . And the higher the pressure is, the smaller of the effect of the pressure on the Debye temperature Θ is. Fig. 4(b) is shown that when the temperature is constant, the Debye temperature Θ increases non-linearly with applied pressures, indicating the change of the vibration frequency of particles under pressure.

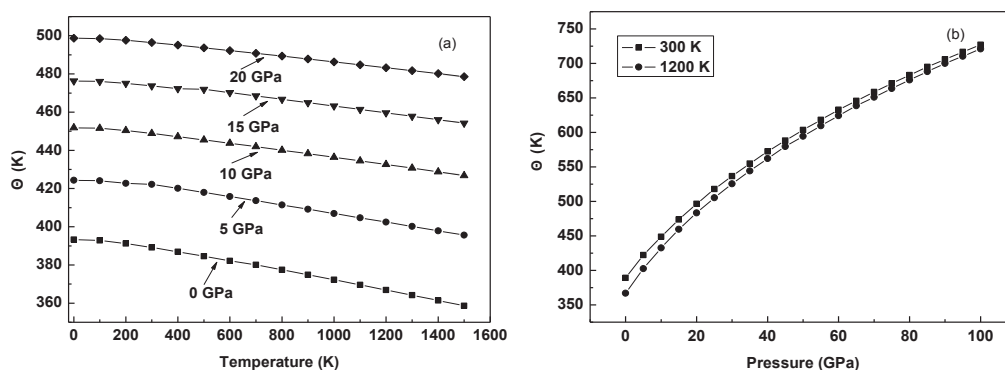


Figure 4: The static variation of the Debye temperature Θ with the temperature at different pressures of $P=0, 5, 10, 15$ and 20 GPa (a), at different temperatures of 300 K and 1200 K (b).

As one of the most important thermodynamic properties of the solid, the heat capacity as a function of temperature and pressure are plotted in Fig. 5. From Fig. 5(a) it can be found that the C_V follows the relationship of the Debye model [$C(T) \propto T^3$] at the low temperature. At high temperatures, the C_V increases monotonously with the temperature and converges to a near-constant value. However, Fig. 5(b) indicates that the heat capacity C_V decreases with the applied pressures. Therefore, Fig. 5 implies that temperature and pressure have opposite influences on the heat capacity and the effect of temperature on the heat capacity is more

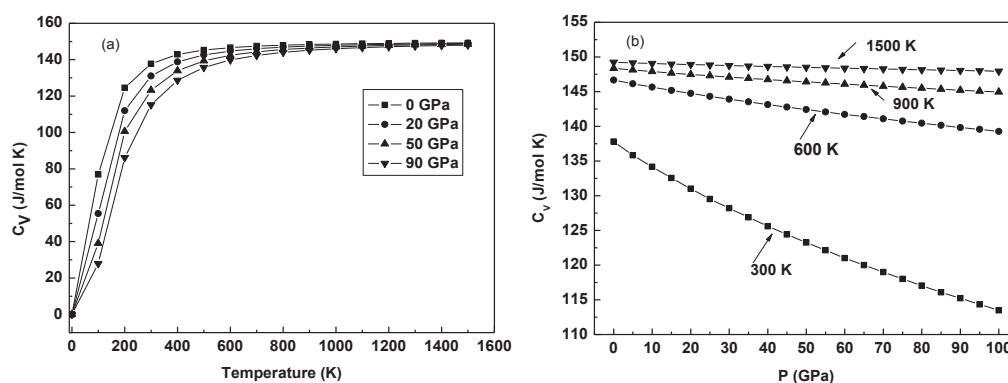


Figure 5: The static variations of heat capacity with (a) temperature at the pressures of 0 GPa, 20 GPa, 50 GPa and 90 GPa, and (b) pressure at the temperatures of 300 K, 600 K, 900 K and 1500 K.

significant than that of pressure on Zr_2Al .

Grüneisen constant g describes the anharmonic effects in the vibrating lattice, and it has been widely used to characterize and extrapolate the thermodynamic behavior of a material at high pressures and temperatures, such as the thermal expansion coefficient and the temperature dependence of phonon frequencies and line-widths. It is also directly related to the equation of state (EOS). The static variation of the Grüneisen parameter with temperature T and pressure P are shown in Fig. 6. It can be observed that at given pressure, the g increases dramatically with the temperature when $T > 500$ K (as shown in Fig. 6(a)) varies almost monotonously with temperature; while at fixed temperature, the decreases dramatically with pressure, and that as the temperature goes higher, the decreases more rapidly with the increase of pressure (see Fig. 6(b)). These results are attributed to the fact that the effect of temperature on the ratio is not as significant as that of pressure, and there will be a large thermal expansion at a low pressure.

The dependence of the thermal expansion a with the temperature and pressure are shown in Fig. 7. From Fig. 7(a) it can be seen that the thermal expansion coefficient also increases with T^3 at lower temperatures and gradually approaches to a linear increase at higher temperatures. Moreover, the variation of the thermal expansion coefficient with temperature is similar to that of C_V . For Fig. 7(b) the effects of the pressure on the thermal expansion coefficient a are very small at low temperature, and as the temperature increases, the effects are becoming obvious. However, it is noted that as the pressure increases, a almost decreases exponentially. This means that there is a large thermal expansion at low pressure which is in accordance with the variation of V/V_0 with pressure. Moreover, the higher the temperature is, the faster the a decreases.

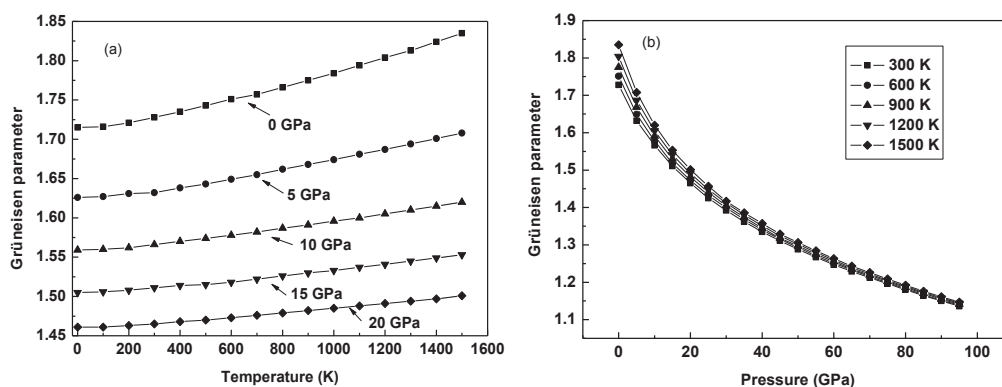


Figure 6: The static variation of the Grüneisen parameter with (a) temperature and (b) pressure.

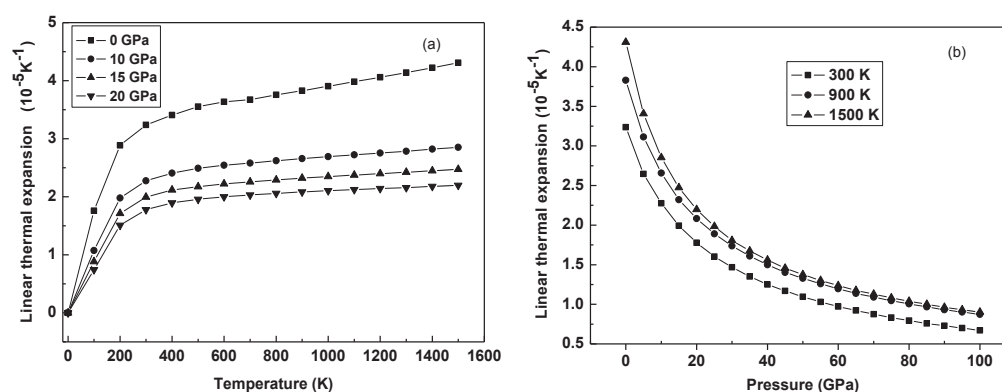


Figure 7: The static variation of the thermal expansion coefficient α with (a) temperature and (b) pressure.

4 Conclusions

The equations of state (EOS) and other thermodynamic properties of hcp structure Zr_2Al are investigated using density functional theory method with the ultrasoft pseudopotential scheme in the frame of the generalized gradient approximation (GGA) under high pressure. It is demonstrated that the ratio c/a of about 1.208 is the most stable structure for hcp Zr_2Al , the calculated zero pressure bulk module B_0 and the pressure derivation of bulk modulus B'_0 from the natural strain EOS and from the quasiharmonic Debye model are about 102.71 GPa and 3.700, 100.52 GPa and 3.736, respectively. Through the quasi-harmonic Debye model, the dependences of the volume compression on pressure and the volume on temperature are successfully obtained, and Furthermore, the high temperature leads to a smaller Debye temperature Θ , a larger heat capacity, Grüneisen parameter g and a bigger thermal expansion

coefficient α , but the high pressure can produce a larger Debye temperature Θ , a smaller heat capacity C_V , a smaller Grüneisen parameter g and thermal expansion coefficient α in the wide range of pressures and temperatures.

Acknowledgments. This work is supported by grants from the National Natural Science Foundation of China under Grant Nos. 11174214 and 20773085, the Specialized Research Fund for the Doctoral Program of Higher Education under Grant No. 20090181110080, the State Key Laboratory of Explosion Science and Technology, Beijing Institute of Technology under Grant No. KFJJ09-02, the National Basic Research Program of China under Grant No. 2010CB731600, as well as, the computational resources provided by the State Key Laboratory of Polymer Materials Engineering of China in Sichuan University and the Virtual Laboratory for Computational Chemistry of CNIC, and the Supercomputing Center of CNIC, Chinese Academy of Science.

References

- [1] Y. K. Vohra and P. T. Spencer, *Phys. Rev. Lett.* 86 (2001) 3068.
- [2] L. E. Edshamar, *Acta. Chem. Scand.* 16 (1960) 20.
- [3] K. Schubert, T. R. Anatharaman, H. O. K. Ata, *et al.*, *Naturwissenschaften* 47 (1960) 512.
- [4] C. G. Wilson and D. Sams, *Acta Crystallogr.* 14 (1961) 71.
- [5] C. G. Wilson and F. J. Spooner, *Acta Crystallogr.* 13 (1960) 358.
- [6] C. G. Wilson, D. K. Thomas, and F. J. Spooner, *Acta Crystallogr.* 13 (1960) 56.
- [7] C. G. Wilson, *Acta Crystallogr.* 12 (1959) 660.
- [8] T. J. Renouf and C. A. Beevers, *Acta Crystallogr.* 14 (1961) 469.
- [9] G. Brauer, *Z. Anorg. Chem.* 242 (1939) 1.
- [10] M. Pöstchke and K. Schubert, *Z. Metallkd.* 53 (1962) 549.
- [11] D. J. McPherson and M. Hansen, *Trans. ASM* 46 (1954) 354.
- [12] T. Wang, Z. Jin, and J. Zhao, *J. Phase Equilibria* 22 (2001) 544.
- [13] A. Peruzzi, *J. Nucl. Mater.* 186 (1992) 89.
- [14] S. N. Tiwari and K. Tangri, *J. Nucl. Mater.* 34 (1970) 92.
- [15] R. J. Kematich and H. F. Franzen, *J. Solid State Chem.* 54 (1984) 226.
- [16] M. Alatalo, M. Weinert, and R. E. Watson, *Phys. Rev. B* 57 (1998) R2009.
- [17] A. Schneider, H. Klotz, J. Stendel, and G. Strauss, *Pure Appl. Chem.* 2 (1961) 13.
- [18] P. Hohenberg and W. Kohn, *Phys. Rev.* 136 (1964) B864; W. Kohn and L. J. Sham, *Phys. Rev.* 140 (1965) A 1133.
- [19] M. C. Payne, M. P. Teter, D. C. Allen, *et al.*, *Rev. Mod. Phys.* 64 (1992) 1045.
- [20] V. Milan, B. Winker, J. A. White, *et al.*, *Int. J. Quantum Chem.* 77 (2002) 85.
- [21] E. Francisco, M. A. Blanco, and G. Sanjurjo, *Phys. Rev. B* 63 (2001) 094107; M. A. Blanco, E. Francisco, and V. Luana, *Comput. Phys. Commun.* 158 (2004) 57.
- [22] J. P. Perdew, K. Burke, and M. Ernzerhof, *Phys. Rev. Lett.* 77 (1996) 3865.
- [23] A. A. Maradudin, E. W. Montroll, G. H. Weiss, and I. P. Ipatova, *Theory of Lattice Dynamics in the Harmonic Approximation* (Academic Press, New York, 1971).
- [24] M. A. Blanco, A. M. Pendás, E. Francisco, *et al.*, *J. Mol. Struct. (Theochem.)* 368 (1996) 245.
- [25] E. Francisco, J. M. Recio, M. A. Blanco, and A. M. Pendás, *J. Phys. Chem.* 102 (1998) 1595.
- [26] M. Flórez, J. M. Recio, E. Francisco, *et al.*, *Phys. Rev. B* 66 (2002) 14411.
- [27] L. Y. Lu, J. J. Tan, O. H. Jia, and X. R. Chen, *Physica B* 399 (2007) 66.

- [28] J. Chang, Y. Cheng, and M. Fu, J. At. Mol. Sci. 1 (2011) 243.
- [29] X. F. Li and Z. L. Liu, J. At. Mol. Sci. 3 (2012) 78.
- [30] X. R. Chen, Z. Y. Zeng, Z. L. Liu, *et al.*, Phys. Rev. B 83 (2011) 132102.
- [31] J. P. Poirier and A. Tarantola, Phys. Earth Planet Int. 109 (1998) 1.
- [32] C. G. Wilson and D. Sams, Acta Ctystallogr. 14 (1961) 71.
- [33] E. Clouet, J. M Sanchez, and C. Sighi, Phys. Rev. B 65 (2002) 094105.
- [34] X. L. Yuan, D. Q. Wei, X. R. Chen, *et al.*, J. Alloys Compd. 509 (2011) 769.
- [35] G. Steinle-Neumann, L. Stixrude, and R. E. Cohen, Phys. Rev. B 60 (1999) 791.
- [36] O. L. Anderson, J Phys. Chem. Solids 24 (1963) 909.
- [37] J. P. Poirier, Introduction to the Physics of the Earth's Interior (Cambridge University Press, Cambridge, UK 2000).